

A method for the direct measurement of the fibre bed compaction curve of composite prepregs

P. Hubert, A. Poursartip*

Composites Group, Department of Metals and Materials Engineering, The University of British Columbia, Vancouver, British Columbia, Canada V6T 1Z4

Received 8 September 1998; revised 13 April 2000; accepted 4 August 2000

Abstract

A method to measure the fibre bed compaction curve directly from composite prepreg is presented. The method was used to measure the compaction curve of unidirectional and quasi-isotropic AS4/3501-6 carbon–epoxy prepregs. Similar compaction curves were obtained in all cases. The compaction curve obtained was used by a finite element process model, COMPRO, to simulate the uniaxial compaction of 8 and 16 ply laminates at different temperatures. The force–displacement response predicted by the model closely matched the experimental results. The method which can be used on both tape and fabric prepregs, has the major advantages of being a direct measure of the prepreg behaviour, and requires no special preparation of the sample. © 2001 Elsevier Science Ltd. All rights reserved.

Keywords: D. Mechanical testing; A. Prepreg; E. Consolidation; E. Resin flow

1. Introduction

Flow and compaction behaviour during autoclave processing of thermoset matrix composites has a significant effect on the final thickness profile, residual stress distribution and distortion of composite structures. The prediction and control of both the mean value and the variability of these effects is a major concern to industry. To address this problem, science based process models have been developed [1–6]. Typically, these models treat the composite as a deformable fibre bed saturated with a curing resin. The resin flow relative to the fibre bed is governed by Darcy's law and is coupled with the compaction behaviour of the fibre bed. At any point in the composite, the total through thickness stress σ is shared by the fibre bed and the resin (Fig. 1). The simple viscoelastic system presented in Fig. 1 implies that during compaction the resin flow and fibre bed compaction are the viscous and the elastic component, respectively. Theoretically, in a very low fibre volume fraction prepreg, or perhaps in a system with ideal straight fibres, the fibre bed carries no through the thickness stress. In practice, the relatively high fibre volume fraction, and the wavy geometry of real fibre beds mean, significant stress can be borne by the fibre bed, especially if there is any loss

of resin. This leads to the following equilibrium relation:

$$\sigma = \bar{\sigma} + P \quad (1)$$

where $\bar{\sigma}$ is the effective stress in the fibre bed and P the resin pressure. The relationship between the effective stress and the fibre bed deformation is given by the fibre bed compaction curve. This parameter is a critical material property input for any flow-compaction model. Compaction curves have been measured by several investigators for carbon fibre beds [7–12] and glass fibre fabrics [13,14]. Kim et al. [15] did numerous experiments on dry and lubricated glass and carbon fibre beds. Gutowski and Dillon [16] propose a “universal” model that fits all the fibre bed compaction curves found in the literature. They emphasize that this model is valid only if the fibre bed configuration is not modified by the condition of the experiment.

The principal difficulty in determining the fibre bed compaction curve is how to measure the response of the fibre bed alone. The resin plays a significant role, and it is difficult to determine the resin pressure P . Therefore typically, the fibre bed is tested in a dry form or is impregnated with silicone oil after dissolving out the polymer matrix. However the act of dissolving the resin out of the prepreg can change the fibre arrangement and could affect the fibre bed compaction behaviour. It is also a time-consuming and tricky operation. The use of a very low viscosity fluid (e.g. $\mu < 0.1$ Pa s) or no fluid, and the loading of the specimen at a very low rate (e.g. < 0.1 mm/min) are steps normally taken

* Corresponding author.

E-mail address: anoush.poursartip@ubc.ca (A. Poursartip).

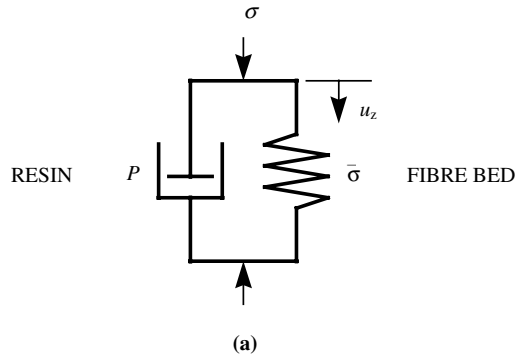


Fig. 1. Analog representation of composite prepreg with the elastic (fibre bed) and viscous response (resin) of compaction.

to minimize the viscous response effects caused by the fluid flow out of the sample. When a wetting fluid is used, the fluid pressure is measured and subtracted from the total applied stress to obtain the fibre bed effective stress.

In the present work, an experimental procedure is presented which allows the measurement of the compaction behaviour directly from the actual prepreg. This technique allows the measurement of the material as is, without any steps that could alter the fibre arrangement in the matrix. In addition, the technique is very simple, and requires little sophisticated instrumentation or equipment. Results obtained for a commonly used composite system are presented, followed by a series of verification simulations.

2. Experimental procedure

The testing apparatus developed to obtain the compaction curve (Fig. 2) is similar to that used in Ref. [7]. With this apparatus, a unidirectional composite specimen is loaded in the vertical direction (z), which is the main deformation

mode of the fibre bed. To obtain a uniaxial testing condition, the deformation in the transverse (y) direction is blocked by the mould walls and the fibres are oriented in the longitudinal (x) direction. Since, the fibres are very stiff in the longitudinal direction compared to the transverse vertical deformation, fibre bed deformation in the longitudinal direction is negligible. The composite is heated and resin is allowed to flow out longitudinally (x direction) in order to get the fibre bed effective stresses at increasing values of compaction strain. The compaction curve of the fibre bed is extracted from the measured displacement (u_z) and applied load (F_z).

A compaction testing fixture was designed and installed on a servo-hydraulic testing machine (Fig. 3(a)). The fixture consists of a top piston that applies the load to the sample, which is constrained laterally (y direction) in a mould (Fig. 3(b)). The gap tolerance between the mould wall and the piston is just enough to provide a sliding fit between the two parts. The fixture was installed in an environmental chamber where the temperature can be controlled from room temperature to 200°C. Heat is applied to the mould by air convection. The temperature of the mould is monitored by two thermocouples located at the top and lower parts of the fixture. The testing fixtures are machined from solid steel, and thus have a relatively high thermal mass. Therefore, once the target temperature is reached, the fixture temperature remains stable during the test. The load applied to the specimen is measured by the load cell of the testing machine. The displacement of the mould is monitored by the testing machine LVDT, which was previously calibrated with a digital micrometer. The tests are conducted under displacement control. This way, the compaction of the specimen is precisely controlled.

The procedure to measure and compute the fibre bed compaction curve is presented in Fig. 4. The method consists of deforming the specimen to increasing levels of displacement. At each increment, the displacement is held

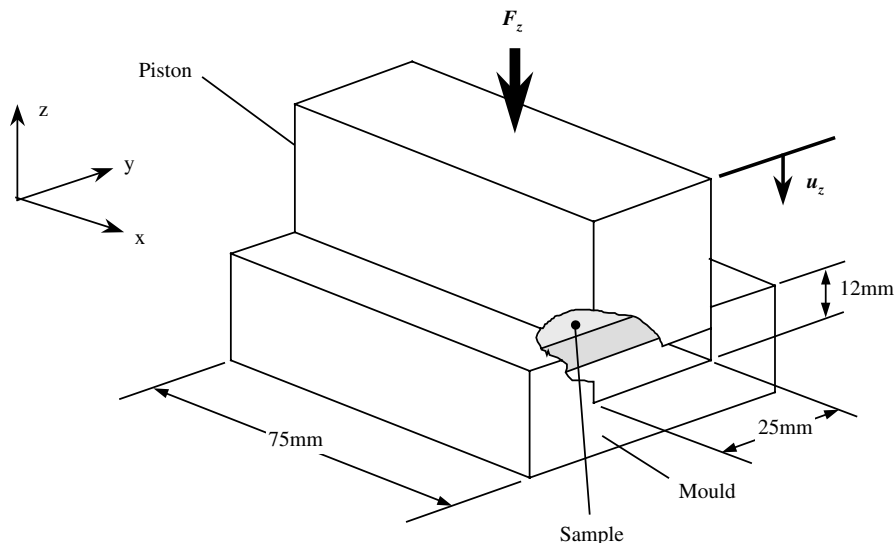


Fig. 2. Schematic of the experimental setup for the fibre bed compaction tests.

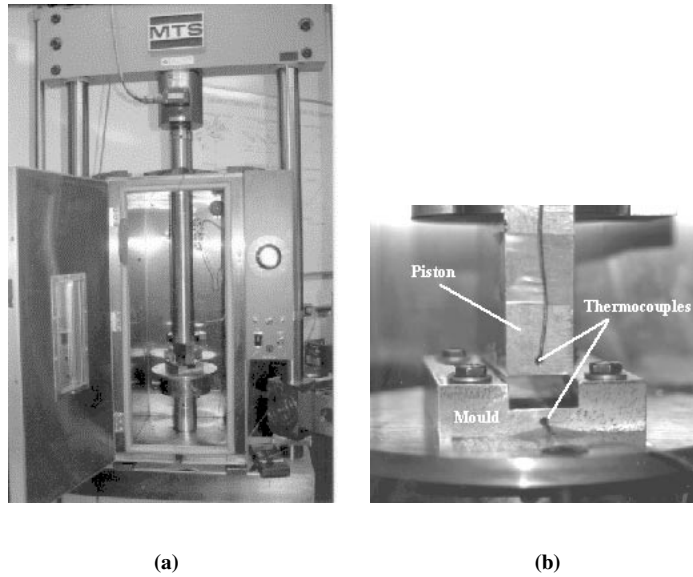


Fig. 3. Photographs of: (a) the compaction fixture as installed in a temperature controlled chamber; and (b) a close-up view of the compaction fixture.

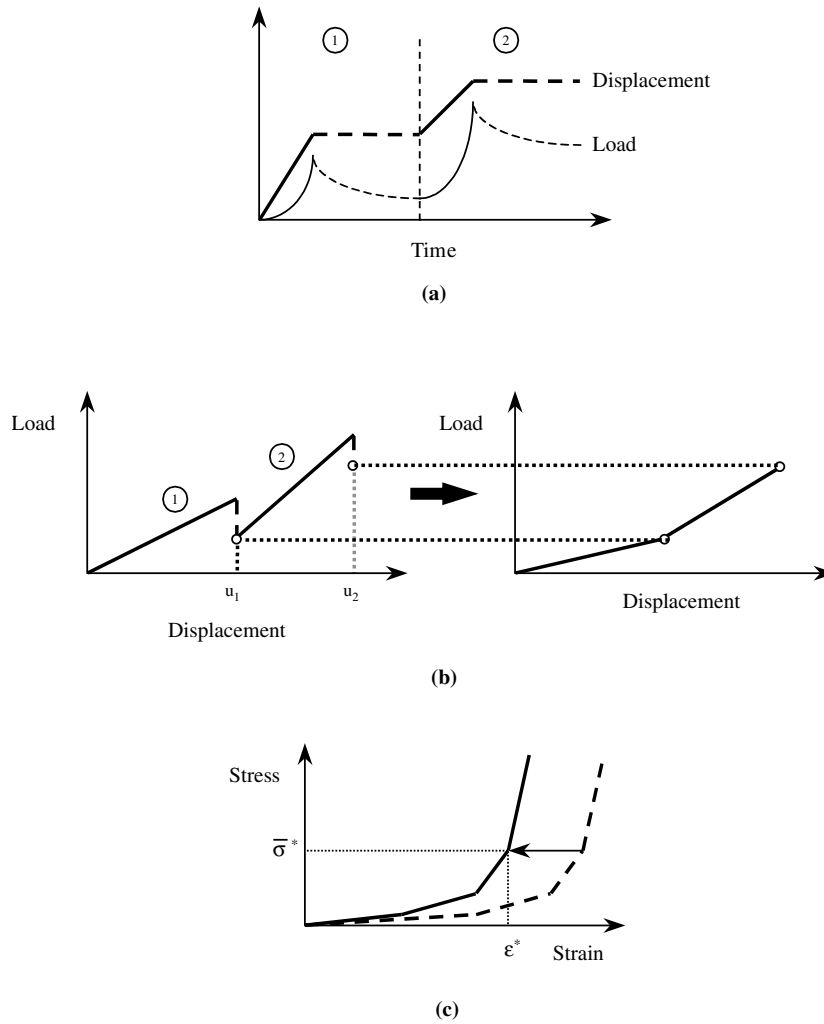


Fig. 4. Compaction curve measurement procedure: (a) deformation is applied in increments until the measured load stabilizes to a constant value; (b) the compaction curve is directly obtained from the load–displacement; and (c) the compaction curve is shifted on the strain axis to pass through a measured compaction test performed under stress control.

Table 1
Total in-plane strains and volumetric strain measured after the compaction tests

Sample	ε_x (mm/mm)	ε_y (mm/mm)	ε_v (mm/mm)
[0]-1	0.00	0.00	-0.17
[0]-2	0.01	0.00	-0.21
[0]-3	0.01	0.00	-0.24
[0]-4	0.00	0.02	-0.19
[0]-5	0.00	0.00	-0.18
[0]-6	0.00	0.01	-0.17
[Q]-1	0.01	0.00	-0.16
[Q]-2	0.01	0.00	-0.18
[Q]-3	0.01	0.01	-0.18
[Q]-4	0.01	0.00	-0.18

constant until the load measured relaxes to a stable value (Fig. 4(a)). Assuming the composite material as a simple viscoelastic system (Fig. 1), the value of the relaxed load will correspond to the elastic response of the material, which is the fibre bed effective stress for a given displacement. By loading the specimen to different displacement levels, the complete fibre bed compaction curve is extracted from the displacements and the relaxed load values at each loading step. From the master loading curve, the relaxed load is plotted against the displacement at each holding step (Fig. 4(b)). Finally, the stress–strain curve obtained from the load–displacement curve is shifted as shown in Fig. 4(c). The calculated stress–strain curve (the dashed curve) is forced to pass through a point $(\varepsilon^*, \bar{\sigma}^*)$. This point is obtained by an independent compaction test at a constant pressure until all the applied stress (σ) is taken by the fibre bed ($\bar{\sigma}^*$) where the final compaction strain (i.e. volumetric strain) is ε^* . This shifting on the strain axis is required since it is very difficult to determine precisely the onset of specimen loading.

The specimens were prepared by laying-up 16 plies of AS4/3501-6 carbon–epoxy prepreg. Six unidirectional $[0]_{16}$ and four quasi-isotropic $[0, +45, -45, 90]_4$ specimens were tested. The specimens length (L) and width (W) were 50 and 25 mm, respectively. The specimens were debulked at room temperature in a vacuum bag. This procedure was required to remove most of the air bubbles between the individual plies. A series of measurements (sample mass and geometric dimensions) were taken before the test. The specimens were wrapped in a thin film of Teflon (thickness of ≈ 0.01 mm) to prevent them from sticking to the fixture. The Teflon film also stops any possible resin flow in the sliding fit between the mould wall and the piston. The deformation of the Teflon film accounts for less than 1% of the specimen deformation in the pressure range of interest ($\sigma < 1$ MPa) and was ignored in the analysis of the results. The specimen final strains (ε_x and ε_y) are determined from the caliper measurements of the specimens length and width before and after the test. The specimen volumetric strain (ε_v) is computed from the resin mass loss during the test. The following expressions are used to calculate the different specimen strains:

$$\varepsilon_x = \frac{L' - L_0}{L_0} \quad \varepsilon_y = \frac{W' - W_0}{W_0} \quad (2)$$

$$\varepsilon_v = \frac{1}{\rho_R} \left(\frac{M_0 - M'}{L_0 W_0 H_0} \right)$$

where ρ_R is the resin density, L_0 , W_0 , H_0 are the initial sample length, width and thickness, respectively, L' , W' , H' are the final sample dimensions, M_0 and M' are the initial and final mass. The testing conditions, namely the temperature and the loading rate, were selected to minimize the viscosity of the resin and to maximize the duration of the

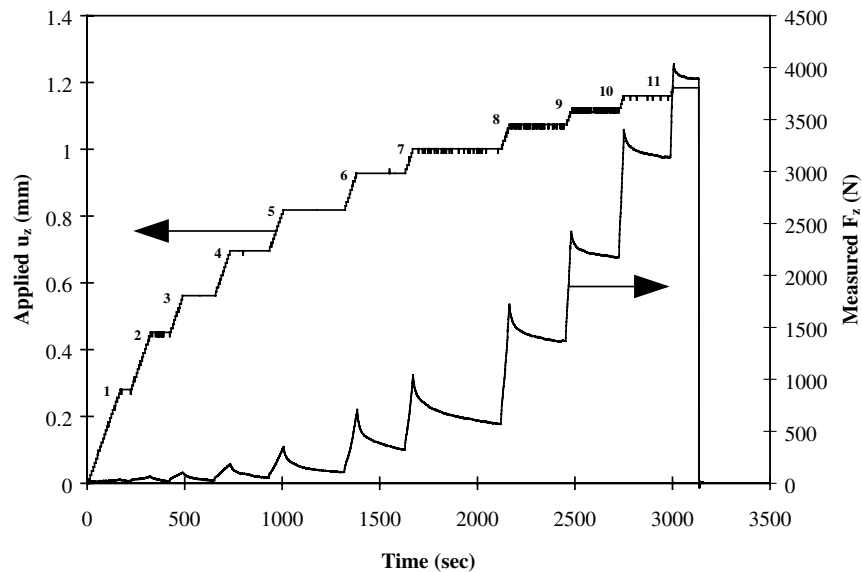


Fig. 5. Applied displacement and measured load variation with time showing the load relaxation at the different displacement increments (1–11).

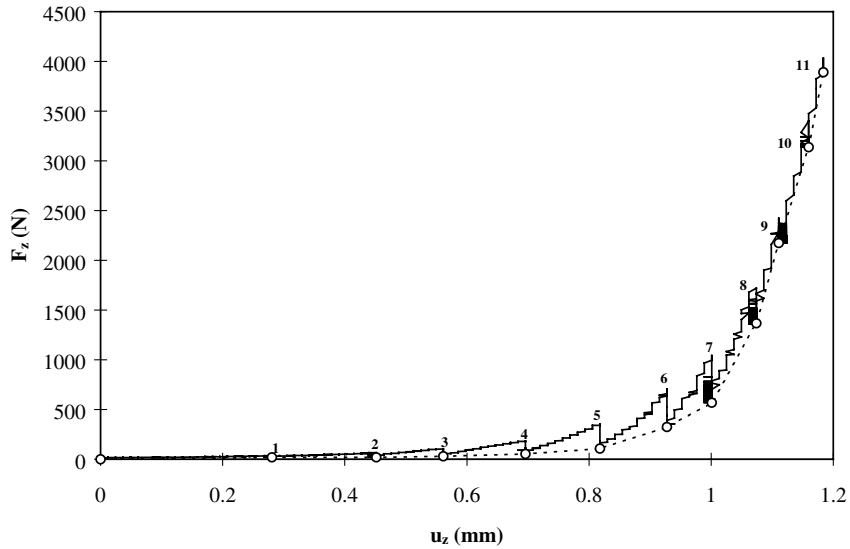


Fig. 6. Load–displacement curve showing the points (1–11) extracted to generate the fibre bed compaction curve.

test before the resin starts to cure. Using the viscosity data for the 3501-6 resin [17], a testing temperature of 100°C and a loading rate of 0.1 mm/min. were chosen. With these conditions, the test duration was between 30 and 60 min which does not allow the resin to cure significantly since viscosity measurement data suggests that the resin viscosity will increase from 0.4–3.5 Pa s, well below the gel point at 1000 Pa s.

3. Results and discussion

The specimen final strains calculated using Eq. (2) are presented in Table 1. In all cases, ϵ_x and ϵ_y were negligible as expected by the physical constraints of the mould and by the fact that the fibres prevented any motion in the long-

itudinal direction. Therefore, the measured vertical deformation of the specimen (ϵ_z) were caused by the volumetric strains which are a consequence of the bleeding of excess resin. A typical variation of the displacement u_z and the applied load F_z with time for the load-hold compaction test is presented in Fig. 5. During each displacement hold period, the load gradually relaxes to a stable level. This behaviour confirms the viscoelastic nature of the material depicted in Fig. 1. To verify that the hold times allowed sufficient load relaxation before loading to the next increment, the following exponential load decay relation was fitted to the force time relaxation data for each time increment:

$$F_Z(t) = (F_0 - F_\infty) e^{-bt} + F_\infty \tag{3}$$

where b is a constant, F_0 is the initial load (when $t = 0$) and F_∞

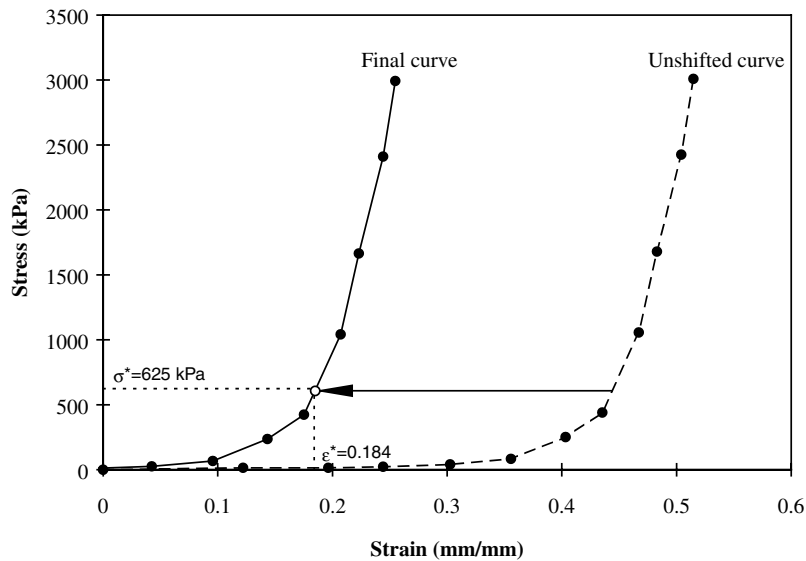


Fig. 7. Compaction curve shift to the measured compaction point $\epsilon^* = 0.184$ and $\bar{\sigma}^* = 625$ kPa.

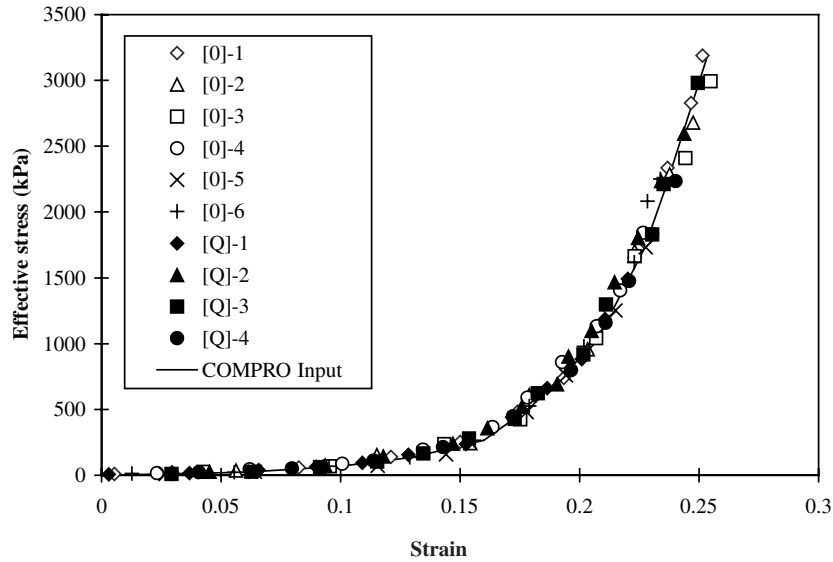


Fig. 8. Compaction curves obtained for all specimens, and fitted curve used in computer simulations.

is the relaxed load (when $t \rightarrow t_{\infty}$). The accuracy of Eq. (3) to fit the load relaxation data was verified by computing the correlation coefficient squared (R^2). For all load increments, R^2 was between 0.95 and 0.99 which indicates a very good fit since $R^2 = 1$ indicates a perfect fit. Using Eq. (3), we found that the difference between F_{∞} and the measured relaxed load was less than 0.1% FSD confirming that the hold times were long enough. The relaxed load increases after each load step. The increase in relaxed load was gradual for steps 1–5 and was much faster for steps 6–11. This directly confirms that the elastic load-bearing capacity of the specimen increases with increasing deformation. This behaviour supports the assumption that the fibre bed behaves as a stiffening spring.

As shown schematically in Fig. 4(b), the fibre bed elastic response can be constructed from the load–displacement curve. The dashed line in Fig. 6 is the generated fibre bed load–displacement curve which is converted into a stress–

strain curve shown in Fig. 7 (dashed curve). The final step consists of shifting the obtained stress–strain curve on the strain axis (Fig. 7) so that the curve passes through the point $(\epsilon^*, \bar{\sigma}^*)$ obtained from an independent compaction test performed under constant stress until full compaction was achieved. For the prepreg studied, this point was measured at $\epsilon^* = 0.184$ and $\bar{\sigma}^* = 625$ kPa during a constant stress compaction of a 16 ply unidirectional sample at 180°C. Under these conditions, the laminate was fully consolidated and the measured volumetric strain (or resin volume loss) corresponds to the fibre bed strain at the applied stress. The fibre bed compaction curves obtained for all specimens are presented in Fig. 8. All tested specimens follow the same master curve, including the quasi-isotropic specimens. This indicates that the transverse compression behaviour of the prepreg is not significantly affected by the lay-up.

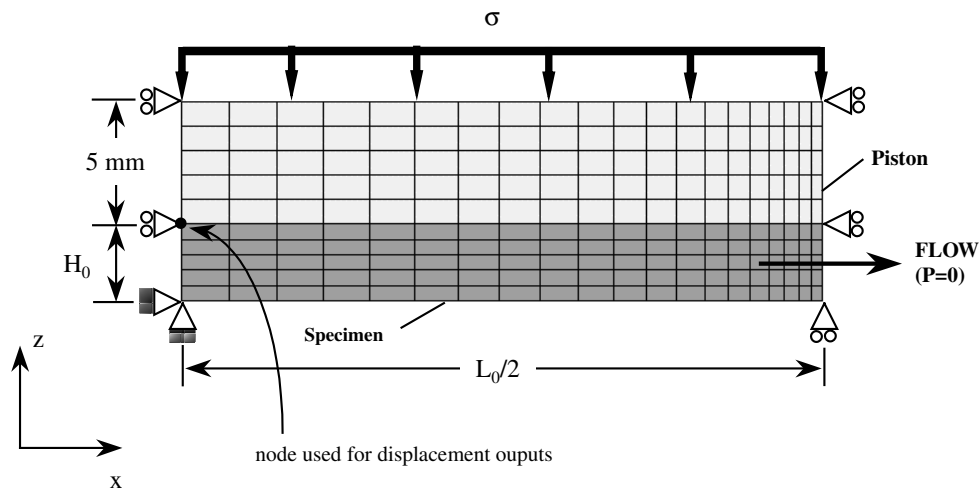


Fig. 9. Finite element model used for the compaction curve validation runs.

Table 2
Comparison between predicted and measured specimen volumetric strains for the validation compaction tests

Sample	Experiment	COMPRO
V100	−0.17	−0.19
V140	−0.18	−0.19
V180	−0.19	−0.19

4. Compaction curve validation

Independent validation tests were conducted to verify the validity of the obtained compaction curves. The tests consisted of using the compaction fixture (Fig. 2) to load a specimen at different temperatures. The specimens were loaded in load control mode to simulate an autoclave condition where a prescribed pressure (rather than a prescribed deformation) is applied to the laminate. The first tests named V100 and V140, were conducted for the following temperatures: 100 and 140°C with an 8 ply AS4/3501-6 [0]₈ laminate at a loading rate of 77 kPa/min to a maximum pressure of 800 kPa. For these tests, the specimen was unloaded after reaching the maximum pressure. A third test named V180 was conducted at a temperature of 180°C with a 16 ply AS4/3501-6 [0]₁₆ laminate at a loading rate of 128 kPa/min to a maximum pressure of 570 kPa. For this test, the pressure was kept constant for 4 min before the specimen was unloaded. The validation procedure consists of a comparison between the measured and predicted load–displacement curve and resin mass losses using a finite element composites processing model (COMPRO) [18].

5. Compaction test finite element model

For each specimen tested, a finite element mesh was constructed. An example of the mesh used is shown in Fig. 9. One half of the specimen was modelled due to the symmetry of the problem. The mesh was divided in two regions: the piston and the specimen. The piston was modelled to reproduce the uniform compaction of the specimen during a compression test. The stiffness and impermeability of the steel piston was achieved by setting the element properties accordingly. The load measured during the real compaction test was applied at the top of the piston as shown in Fig. 9. The sliding motion of the piston was ensured by vertical sliding displacement conditions. Resin flow out of the laminate was permitted by setting the resin pressure to atmospheric at the right edge of the specimen (Fig. 9). The temperature was set to be constant and uniform in the piston and at the boundaries of the specimen during the entire simulation. The compaction curve used for the simulation is shown in Fig. 8. The vertical displacement (u_z) extracted from the simulation corresponds to the value at the node indicated in Fig. 9. The predicted displacements were confirmed to be uniform along the length of the specimen, as in the actual compression test.

6. Discussion

Table 2 compares the volumetric strains predicted by the flow-compaction model with the experimental data. In Figs. 10 and 11, the compaction predictions are compared with the experimental results at 100 and 140°C. In both cases, the agreement between the numerical and the experimental data

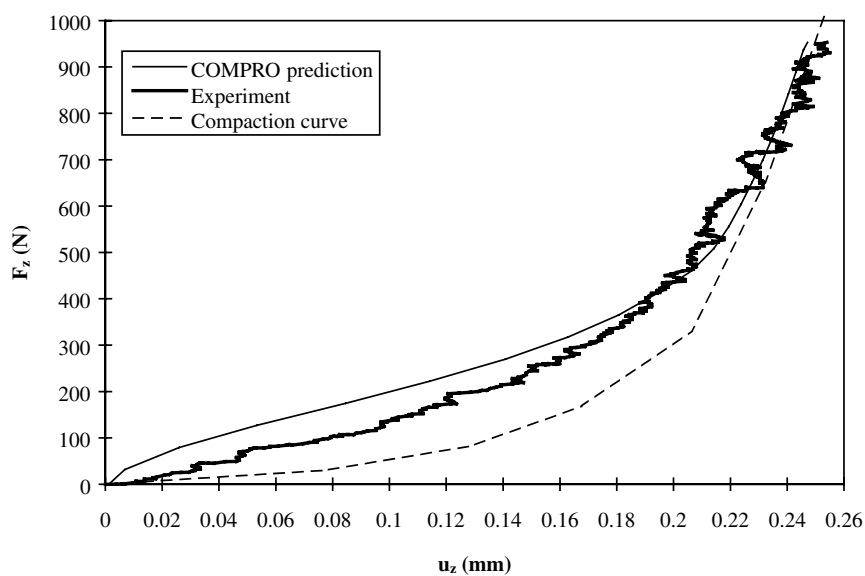


Fig. 10. Predicted and measured load–displacement behaviour of a AS4/3501-6 [0]₈ laminate subjected to a load controlled compaction test at a loading rate of 77 kPa/min to 800 kPa and a temperature of 100°C (sample V100). The fibre bed elastic compaction curve is shown for reference.

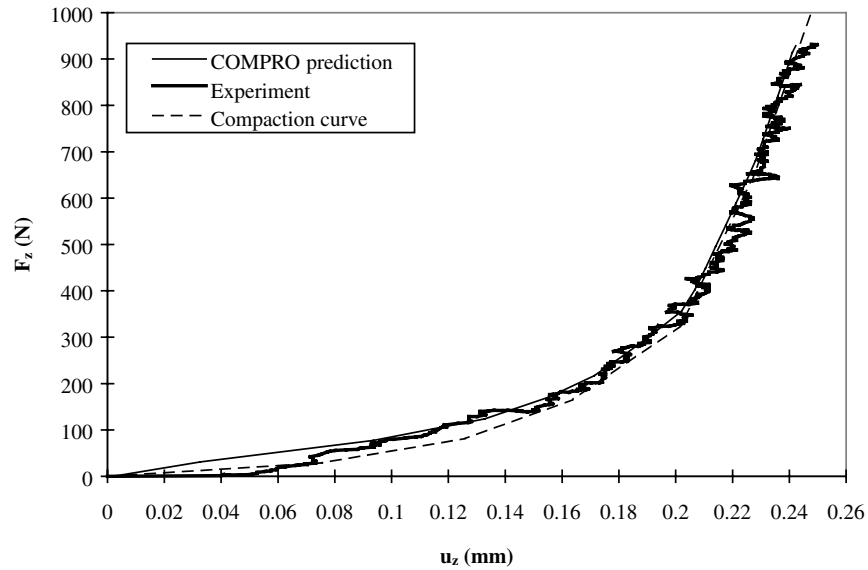


Fig. 11. Predicted and measured load–displacement behaviour of a AS4/3501-6 [0]₈ laminate subjected to a load controlled compaction test at a loading rate of 77 kPa/min to 800 kPa and a temperature of 140°C (sample V140). The fibre bed elastic compaction curve is shown for reference.

is very good. The load predicted by the model for the test at 100°C (Fig. 10) is slightly higher in the early stages of compaction ($u_z < 0.2$ mm). The actual fibre bed compaction curve was added to the graph for reference. As expected, during the early stages of compaction, where the fibre bed elastic stiffness is very low, the behaviour is dominated by viscous effects: the difference between the compaction curve and the load–displacement curve is important. During this phase, the bulk of resin flow is taking place as indicated by the large displacement change. The final stage of compaction is controlled by the fibre bed elastic response as the fibre bed stiffness increases dramatically. By increasing the

temperature, the viscous effects become less important. This is shown by the smaller difference between the compaction curve and the load–displacement curve for the 140°C test (Fig. 11) compared to the 100°C test (Fig. 10). The experimental results confirm that as the resin viscosity decreases the load–displacement curve of the sample approaches the load–displacement curve of a purely elastic fibre bed. Fig. 12 shows the result for the test at 180°C and again very good agreement between the model prediction and the experiment was found. In this case, it is important to realize that the higher loading rate used for V180 significantly increases the viscous effects even with the reduction

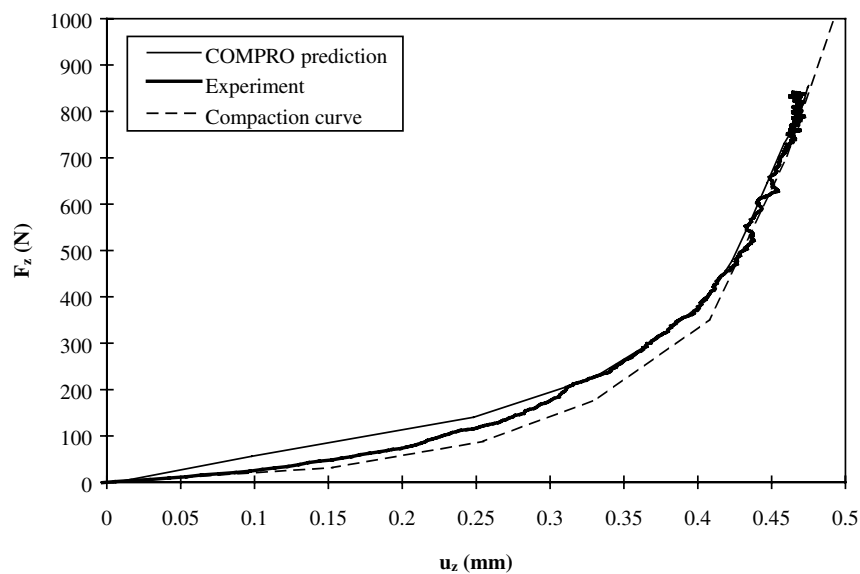


Fig. 12. Predicted and measured load–displacement behaviour of a AS4/3501-6 [0]₁₆ laminate subjected to a load controlled compaction test at a loading rate of 128 kPa/min to 570 kPa and a temperature of 180°C (sample V180). The fibre bed elastic compaction curve is shown for reference.

of resin viscosity caused by the higher temperature. This is shown by the slightly higher offset between the compaction curve and the load–displacement curve for V180 compared to V140. Nevertheless, the good agreement found for all validation tests confirm that the compaction curve for AS4/3501-6 prepreg shown in Fig. 8 describes adequately the actual compaction of the material in typical processing conditions.

7. Conclusions

The method presented here is simpler than other methods and has the added advantage that it directly provides the actual compaction curve of the unmodified prepreg. The method does not require any complex and delicate sample preparation that could alter the fibre bed structure and therefore the measured compaction curve. This method can be applied to other types of composite systems including woven or non-woven fabrics. The compaction curve obtained can be used in process models to predict the laminate compaction behaviour under different processing conditions.

Acknowledgements

This work was supported by funding from the Natural Sciences and Engineering Research Council of Canada. We would also like to gratefully acknowledge the significant interaction and support from our colleagues at The University of British Columbia, The Boeing Company and Integrated Technologies Inc. We would like to acknowledge the contribution of Mrs. Laura Petrescue for her work on the measurement of the compaction curves.

References

- [1] Hubert P, Poursartip A. A review of flow and compaction modelling relevant to thermoset matrix laminate processing. *Journal of Reinforced Plastics and Composites* 1998;17(4):286–318.
- [2] Davé R. A unified approach to modeling resin flow during composite processing. *Journal of Composite Materials* 1990;24(1):22–41.
- [3] Gutowski TG, Morigaki T, Cai Z. The consolidation of laminate composites. *Journal of Composite Materials* 1987;21(2):172–88.
- [4] Hubert P, Vaziri R, Poursartip A. A two dimensional flow model for the process simulation of complex shape composite laminates. *International Journal of Numerical Methods in Engineering* 1999;44(1):1–26.
- [5] Loos AC, Springer GS. Curing of epoxy matrix composites. *Journal of Composite Materials* 1983;17(2):135–69.
- [6] Young W-B. Resin flow analysis in the consolidation of multi-directional laminated composites. *Polymer Composites* 1995;16(3):250–7.
- [7] Gutowski TG, Kingery J, Boucher D. Experiments in composites consolidation: fiber deformation. *Society of Plastic Engineers. Annual Technical Conference*, 1986. p. 1316–20.
- [8] Gutowski TG, Cai ZD, Kingery J, Wineman SJ. Resin flow/fiber deformation experiments. *SAMPE Quarterly* 1986;17(4):54–58.
- [9] Gutowski TG, Cai Z, Bauer S, Boucher D, Kingery J, Wineman SJ. Consolidation experiments for laminate composites. *Journal of Composite Materials* 1987;21(7):650–69.
- [10] Davé R, Kardos JL, Dudukovic MP. A model for resin flow during composite processing: part 2-numerical analysis for unidirectional graphite/epoxy laminates. *Polymer Composites* 1987;8(2):123–32.
- [11] Lam RC, Kardos JL. The permeability and compressibility of aligned and cross-ply fiber beds during processing of composites. *ANTEC* 1989;89:1408–12.
- [12] Skartsis BK, Kardos JL. Resin flow through fiber beds during composite manufacturing processes. Part II: numerical and experimental studies of Newtonian flow through ideal and actual fiber beds. *Polymer Engineering and Science* 1992;32(4):231–9.
- [13] Pierce N, Summerscales J. The compressibility of a reinforcement fabric. *Composites Manufacturing* 1995;6(1):15–21.
- [14] Saunders RA, Lekakou C, Bader MG. Compression and microstructure of fibre plain woven cloths in the processing of polymer composites. *Composites Part A* 1998;29A:443–54.
- [15] Kim YR, McCarthy SP, Fanucci JP. Compressibility and relaxation of fiber reinforcements during composite processing. *Polymer Composites* 1991;12(1):13–19.
- [16] Gutowski TG, Dillon G. The elastic deformation of lubricated carbon fiber bundles: comparison of theory and experiments. *Journal of Composite Materials* 1992;26(16):2330–47.
- [17] Hubert P. Aspects of flow and compaction of laminated composite shapes during cure. PhD thesis, The University of British Columbia, Vancouver, British Columbia, Canada, 1996.
- [18] Hubert P, Johnston A, Poursartip A, Vaziri R. A two-dimensional finite element processing model for FRP composite components. *Proceedings of the 10th International Conference on Composite Materials (ICCM-10)*. Whistler, British Columbia, August 1995. p. 149–56.